Chem Soc Rev

Self-assembling small molecules for the detection of important analytes

Journal:	*Chemical Society Reviews*
Manuscript ID:	CS-TRV-05-2014-000161.R1
Article Type:	Tutorial Review
Date Submitted by the Author:	10-May-2014
Complete List of Authors:	Ren, Chunhua; College of Pharmacy, Nankai University, Zhang, Jianwu; Southern medical university, Chen, Minsheng; Southern medical university, Yang, Zhimou; The Key Laboratory of Bioactive Materials, Ministry of Education,

Cite this: DOI: 10.1039/c0xx00000x

www.rsc.org/xxxxxx

ARTICLE TYPE

Self-assembling small molecules for the detection of important analytes

Chunhua Ren[a], Jianwu Zhang[b], Minsheng Chen[b], and Zhimou Yang*[a]

Received (in XXX, XXX) Xth XXXXXXXXX 20XX, Accepted Xth XXXXXXXXX 20XX
DOI: 10.1039/b000000x

Nano-materials formed by the self-assembly of small molecules are very promising for drug delivery, regenerative medicine, and detection of important analytes due to their unique properties, such as self-assembled multivalency, biocompatibility, and fast responses to external stimuli. This tutorial review focuses on their applications in detection of important analytes. Self-assembling small molecules can show fast responses to external stimuli. Therefore, the gel-sol/sol-gel phase transitions of supramolecular hydrogels that can be easily identified by naked eyes have been applied for the detection of enzymes and enzyme-involving analytes. The supramolecular hydrogels can also provide semi-wet environments that can retain the activity of enzymes and recognition property of molecular probes. Thus, they provide good platforms for the detection of many biologically and environmentally important analytes. Besides, self-assembling small molecules show big differences in fluorescence or F-NMR signal between their self-assembled and un-assembled stages. Such small molecules can be rationally designed through the integration of fluorescent dyes or fluorine containing molecules in the self-assembling small molecules. Therefore, extensive recent research efforts have been paid to explore their detection application based on the dis-assembly triggered fluorescence/F-NMR signal turn on or the self-assembly/aggregation induced fluorescence turn on. We believe that the research efforts paid to this field will ultimately lead to the development of useful nano-materials for detection applications.

Key Learning Points:

1. Detection applications of supramolecular hydrogels based on gel-sol/sol-gel phase transition that can be easily identified by naked eyes.
2. The advantages of using supramolecular hydrogels for sensing applications.
3. The difference in fluorescence or F-NMR signal of small molecules between self-assembled and un-assembled stages.
4. Challenges in using self-assembling small molecules for detection applications.

1. Introduction

Nature is composed of vast arrays of well-organized functional nanostructures from the self-assembly of monomeric building blocks, such as lipid bilayer, tubulin assembly, and DNA double helix.[1] Inspired by these functional nanostructures, materials scientists have developed many supramolecular nanomaterials through the self-assembly of simple small molecules (molecular self-assembly).[2-7] Molecular self-assembly is a spontaneous association of individual small molecular components into well-ordered structures assisted by non-covalent interactions, such as hydrogen bond, π-π interaction, hydrophobic interaction, and charge interaction. Through molecular self-assembly, small molecules spontaneously associate into adaptable and dynamic supramolecular structures including nanofibers, nanotubes, and nanoparticles.[8-12]

Among the reported supramolecular nano-materials, those based on amino acids, sugars, and peptides are probably the most extensively investigated due to their ease of design and synthesis, biocompatibility, and degradability.[13-16] In order to trigger the self-assembly of small molecules and the formation of supramolecular nano-materials, external stimuli are usually needed.[17] These stimuli are used to decrease the solubility of the small molecules or to produce them by chemical or enzymatic reactions. For example, cooling down a hot water solution of hydrogelator to room temperature will result in nanofiber and supramolecular hydrogel formation. Biocompatible stimuli to form supramolecular nano-materials hold advantages for their biomedical applications, which are actively investigated in recent years.[12, 18, 19] The supramolecular nanomaterials are very promising in diverse applications such as drug delivery,[20] analytes detection,[21, 22] cell culture,[13] immune response boosting,[23] cancer cells and bacterial inhibitions,[24, 25] etc.

Fluorescence detection is a cost-effective, real-time, highly sensitive and specific methodology to detect important analytes and monitor biological events. Many specific probes based on nano-materials and organic dyes have been developed.[21, 26, 27] Recently, supramolecular nano-materials based on self-assembling small molecules emerge as novel and promising materials for such application, because they are naturally occurring building blocks to construct biological systems. More importantly, they show fast and specific responses to many environmentally and biologically important analytes. Taken the

property of dis-assembly triggered fluorescence turn on of conventional dyes,[28] aggregation-induced emission (AIE) of AIE dyes,[29] or environment change-induced fluorescence turn on of environment sensitive dyes,[30, 31] these nano-materials have been applied for the detection of enzymes, metal ions, proteins, etc. In this paper, we summarize part of recent research efforts to develop such nano-materials and their applications in detection of important analytes.

2. Self-assembled supramolecular hydrogels for detection applications

Supramolecular hydrogel emerges as a novel kind of hydrogel and nano-materials in early 1990s.[17, 32] It is a kind of physical gel formed by the self-assembly of small molecules that can show rapid responses to external stimuli. For example, sol-gel or gel-sol phase transitions can be manipulated by pH changes or enzyme triggers. Such kind of transitions can be easily identified by naked eyes, which has been developed into simple assays for rapid screening of enzymes and enzyme-involving species. Besides, supramolecular hydrogel, as an intermediate between aqueous solution and dry solid, provides semi-wet environments that possess several advantages for the detection application: (i) it provides suitable environment to keep the bioactivity of biomacromolecules such as enzymes, (ii) artificial receptors could be physically entrapped in the matrix and their molecular recognition abilities can be retained under such semi-wet conditions, (iii) miniaturization and array-type of arrangement of the hydrogel is feasible for high-throughput sensing. Taken together, supramolecular hydrogels can therefore be developed into useful platforms for detection of enzymes, inhibitors of enzymes, metal ions, and others.

2.1 Detection of enzymes and enzyme-involving analytes based on the gel-sol/sol-gel phase transitions

Enzymes play an important role in biological processes. The over-expression and relative abundance of certain enzymes is a trademark of diseases. For example, over-expressed cathepsins and matrix metalloproteases (MMPs) are usually found in cancers.[33] These enzymes are attractive targets for the development of theranostics for diseases. The inhibitors of these enzymes may also be developed into useful therapeutic agents. Therefore, there is an increasing need to develop enzyme-responsive nano-materials for the detection of enzymes and inhibitors of enzymes.

Hydrolysis and digestion enzymes can cleave hydrophilic fragments from precursors of self-assembling small molecules (e.g. molecular hydrogelators), leading to the formation of hydrogelators and hydrogels. Based on this principle, Xu and co-workers had reported on a simple assay based on the hydrogelation of small molecules for detecting inhibitors of enzymes.[34] As shown in Fig. 1A, upon being catalyzed by a specific enzyme, the precursor transformed into a hydrogelator and further formed a hydrogel through self-assembly. When inhibitors competitively bind with the active site of the enzyme, the conversion of the precursor was blocked and no hydrogel formations occurred. Therefore, a failure of the macroscopic sol–gel transition reported a possible inhibitor of the enzyme. This process had been applied for the detection of inhibitors of acid phosphatase. As shown in Fig. 1B, the acid phosphatase catalyzed the conversion of **1** to **2** and led to hydrogelation at pH~6.0 and 37 ℃, the event of hydrogelation could indicate the activity of inhibitors for the acid phosphatase. Pamidronate disodium, Zn^{2+}, and sodium orthovanadate (Na_3VO_4) were chosen to estimate their minimum inhibition concentrations for the acid phosphatase. Three compounds were mixed with the enzyme firstly at a series of concentrations, respectively. Solution of **1** was then added 10 minutes later. After an additional 30 minutes, the sol–gel phase transition was used to determine the minimum inhibition concentration of the compounds. For example, from the changes of rows 2 in Fig. 1C, they observed that the minimum inhibition concentration of pamidronate disodium for the acid phosphatase was about 33 mM. This approach could be adapted easily into a parallel assay to allow many inhibitors to be tested efficiently.

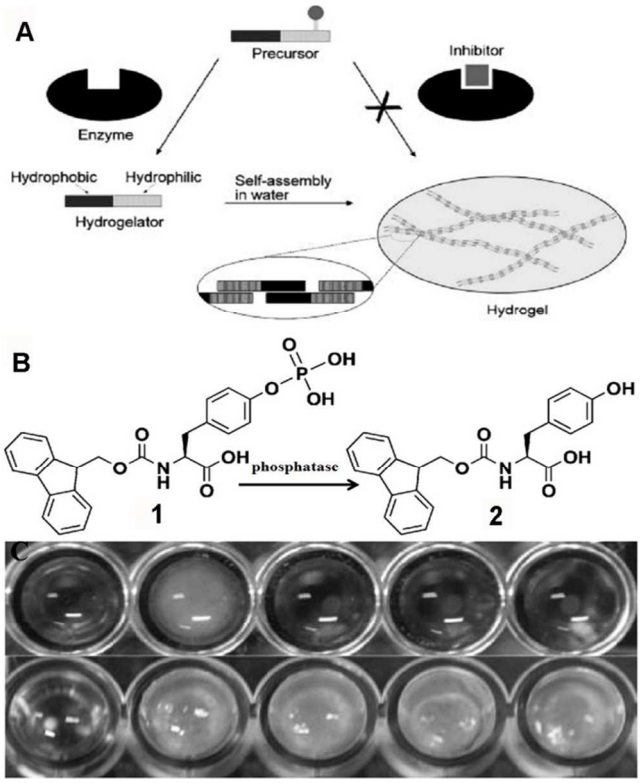

Fig. 1. A) The illustration of the design for identifying inhibitors of an enzyme by hydrogelation, B) The chemical structures of the molecules for hydrogelation and the schematic gelation process catalyzed by the acid phosphatase, C) Results of activities of inhibitors: row 1) Left to right: sol. of **1**; sol. of **1** and enzyme; sol. of **1** and enzyme + pamidronate; sol. of **1** and enzyme + Zn^{2+}; and sol. of **1** and enzyme + Na_3VO_4 ([pamidronate]~[Zn^{2+}]~[Na_3VO_4]~33 mM); row 2) sol. of **1** and enzyme + pamidronate (Left to right, conc. ~33; 3.3; 0.33; 0.033; 0.0033 mM)

Using a similar strategy, McNeil and co-workers had also developed a modular system for detecting protease activity *via* enzyme-triggered gel formation.[35] As shown in Fig. 2A, an enzyme-triggered cleavage at the N-terminus of a peptide gelator, which separated the protease-specific recognition sequence from the gelator, represented a general and modular strategy for detecting enzymatic activity *via* gelation. A dipeptide conjugated *p*-aminobenzoic acid (3), PABA-(D-F_5Phe)-(D-Phe)-NH_2 with a

critical gel concentration (cgc) of 1.7 mM was screened as an efficient peptide-based gelator (Fig. 2B). D-Amino acids were used for their resistance to proteolysis. An oligo(ethylene glycol) unit and three hydrophilic D-amino acids (PEG_4-(D-Arg)-(D-Arg)-(D-Ser)-Pro) were added to the N-terminal end of the recognition sequence as the solubility factor to increase solubility and prevent gelation. The recognition sequence of thrombin (Leu-Thr-Pro-Arg) was initially selected as the linker between the solubility factor and the gelator, which resulted in a thrombin-selective compound. The resulting compound was treated with thrombin (50 nM) in buffer (400 mL, 100 mM PBS, 10% DMSO, pH = 7.2). Within 10 min, a translucent gel was observed (Fig. 2C). The lowest concentration of thrombin that could be detected using this method was 400 pM, indicating that the system functioned at physiological concentrations. The gelator could also be used to create artificial clotting in human blood plasma deficient with fibrinogen. As shown in Fig. 2D, an opaque gel was observed within 2 h after adding thromboplastin to the thrombin-selective compound in fibrinogen-deficient blood plasma. Using the same gelator and solubility factor but simply changing the recognition sequence, two additional proteases were targeted: (recognition sequence of Ala-Ala-Pro-Phe for chymotrypsin and that of Asp-Ala-Phe-Glu for endoproteinase Glu-C(Staphylococcus aureus Protease V8). As shown in Fig. 2E, gelation was observed to be specific to each enzyme based solely on the recognition sequence. Moreover, the enzyme concentrations (50 nM) were also physiologically relevant. These results demonstrated that the modular system was quite general to other proteases and might lead to facile assays for detection and diagnosis of disease-relevant proteases.

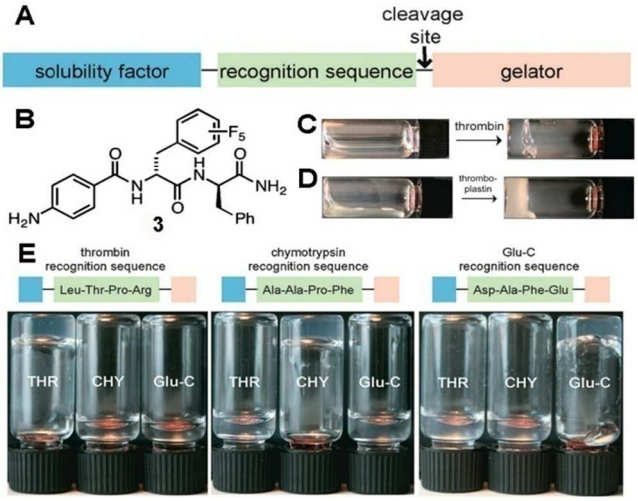

Fig. 2. A) Design strategy of a modular sensor for enzymatic activity based on gelation, B) Chemical structure of the gelator (**3**), C) A clear gel was observed within 10 min by adding thrombin (50 nM) to thrombin-selective pro-gelator in buffer, D) An opaque gel was observed within 2 h by adding thromboplastin to the thrombin-selective pro-gelator in fibrinogen-deficient blood plasma (photo was taken after 20 h), E) Each vial contained ~4 mM of the indicated compound and 50 nM enzyme in buffer where THR = thrombin, CHY = chymotrypsin, and Glu-C = Staphylococcus aureus Protease V8

Many enzymatic reactions will generate acid or base, which changes the pH value of environments and triggers the self-assembly of molecular hydrogelators. Using this strategy, Zhang and co-workers constructed a simple visual assay for glucose detection.[36] As shown in Fig. 3A, glucose could be transferred to gluconic acid by the catalysis of glucose oxidase (GOx). The generated gluconic acid was able to trigger the protonation of the peptide building blocks, thus regulating their self-assembly behaviors. As shown in Fig. 3B, gelator **4** was composed of an aspartic acid residue and a naphthalene–diphenylalanine (Nap–FF) segment that was prone to self-assembly. It was firstly dissolved well at a pH of 10 to form a homogeneous solution (2.5 mg mL^{-1}, 4.2 mM in Fig. 3D-a). After the addition of GOx (1 mg, 100–250 U mg^{-1}) and glucose (10 mg, 0.056 mM), a self-assembled hydrogel was obtained about 40 min later because the pH value of the system decreased from 10 to about 4.2. Opposite to the sol-gel phase transition by using gelator **4** terminated at carboxylic acid, a gel-sol phase transition could be achieved by using a gelator terminated at amine group (Fig. 3C). Gelator **5** could form a self-assembled hydrogel at a pH of 10 if the solution concentration was higher than 5 mg mL^{-1} (6.67 mM, Fig. 3D-c). As shown in Fig. 3D-d, the gel would change to a clear solution about 90 min. later after the addition of GOx (1 mg) and glucose (0.056 mmol) due to the pH value decrease. Because this glucose metabolism regulated self-assembly was based on the oxidation of glucose, the strategy developed by Zhang et al. could therefore be used as a simple visual biosensor for glucose detection.

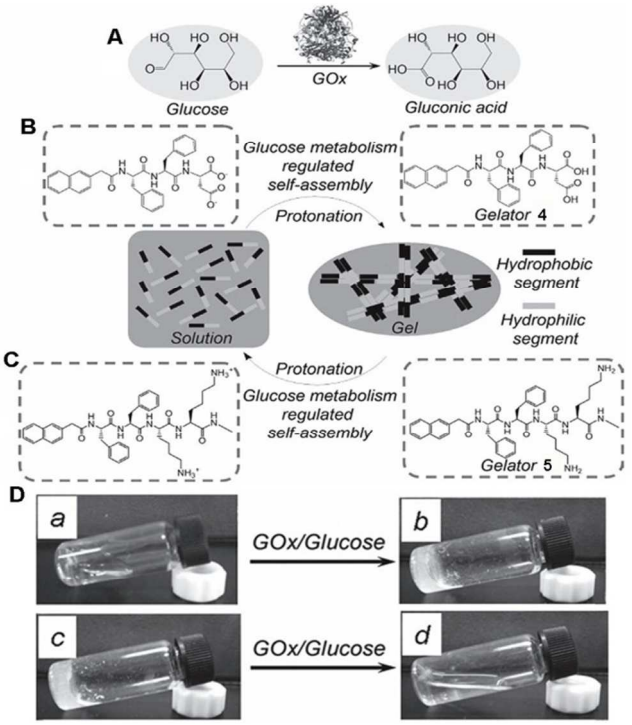

Fig. 3. A) The schematic illustration of the GOx catalyzed glucose metabolism and gluconic acid production, B, C) Glucose metabolism regulated self-assembly of gelators **4** and **5**, D) Glucose metabolism regulated the self-assembly of gelator **4** from an aqueous solution (a) to a hydrogel (b) and that of gelator **5** from a hydrogel (c) to an aqueous solution (d)

2.2 Hydrogels as semi-wet platforms for the detection of enzymes, metal ions, and other analytes

Optical sensors and probes have been widely developed to detect

important analytes, and they can be immobilized on a solid support such as a polymer or glass substrate to yield convenient and high-throughput sensors. However, their binding and/or sensing ability is frequently suppressed after being immobilized to the solid support, compared with that in homogeneous solutions. This disadvantage hinders their development as high-throughput recognition chips. Supramolecular hydrogels are an intermediate between aqueous solution and dry solid. They can provide semi-wet environments for the immobilization of biosensors with the retaining of their original binding function. The semi-wet environment was also beneficial to proteins such as enzymes because the activity of proteins can be mostly retained in hydrogels. Therefore, supramolecular hydrogel has been regarded as a promising molecular recognition chip for convenient and high-throughput assay for screening of enzymes, proteins, and other important analytes.

Hamachi group reported on the first successful attempt to develop a supramolecular hydrogel as a semi-wet peptide/protein microarray.[37] As shown in Fig. 4A, the supramolecular hydrogelator **6** consisted of a glycosylated amino acid scaffold. The amphiphilic molecule provided a bimolecular layer which was stabilized through both the tight packing of the hydrophobic tails and a well-developed network of multiple hydrogen-bonding amide units. The thin fibres further entangled to give thick fibrils. A macroscopic hydrogel formed when the thick fibrils entangled again to form micro-cavities with water molecules being efficiently immobilized. Aqueous cavities created in the gel matrix were a suitable semi-wet reaction medium for enzymes, whereas the hydrophobic domains of the fiber were useful as unique sites for monitoring the reaction.

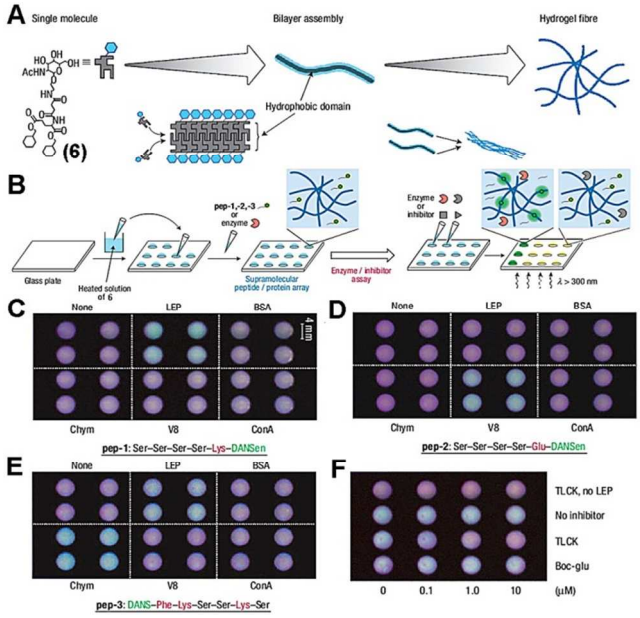

Fig. 4. A) Schematic representation of the hierarchal molecular assembly of ***6*** to form a supramolecular hydrogel, B) Preparation scheme of the supramolecular peptide/protein array (enzymatic reaction leads to the production of the free fluorescent dye and strong fluorescence after its binding to nanofibers), C–E) Fluorescent enzyme activity assay using a supramolecular hydrogel-based peptide chip, F) Assay of LEP inhibitors using supramolecular hydrogel-based protein chip

Semi-wet peptide/protein chips were then constructed using the supramolecular hydrogel. As shown in Fig. 4B, they firstly prepared a supramolecular peptide gel array of gelator **6** on a glass plate. The pep-1,-2,-3 and enzymes were subsequently added to gel spots. The peptide bond between the amino acid and 5-dimethylaminonaphthalene-1-(N-2-aminoethyl) sulphonamide (DANSen) was cleaved by the enzymes, and the resultant DANSen shifted from the aqueous cavity of the hydrogel to the hydrophobic domain of nanofibers because of DANSen's strong hydrophobicity. The binding to nanofibers caused the fluorescence intensity increase for the environmentally sensitive DANSen. The color change in fluorescence of the gel could therefore be visually monitored. For example, when a hydrophilic pentapeptide (pep-1) bearing lysine (Lys) and DANSen at the C-terminal was used as a specific substrate for lysyl-endopeptidase (LEP), a bright emission appeared only at spots injected with LEP (Fig. 4C). Similar results were observed in the case of pep-2, a substrate specific for V8-protease (Fig. 4D) and in the case of pep-3 having cross-reactivities for Chym and LEP (Fig. 4E). These results indicated that the peptide-hydrogel array could be applied to distinguish the protein character based on its enzymatic activity.

The protein-gel chip could also be used to screen inhibitors of enzyme and discriminate levels of the inhibition ability in a high-throughput manner. As shown in Fig. 4F, the gel spot showed a bright green emission in the absence of inhibitors, whereas the emission from spots containing the inhibitor N^{α}-tosyl-lysine chloromethylketone (TLCK) became smeared, depending on the inhibitor concentration. In contrast, spots containing another inhibitor Boc-glu, which was not potent for LEP, remained brightly fluorescent. This array system overcame several drawbacks of conventional protein chips, and thus could have potential applications in pharmaceutical research and diagnosis.

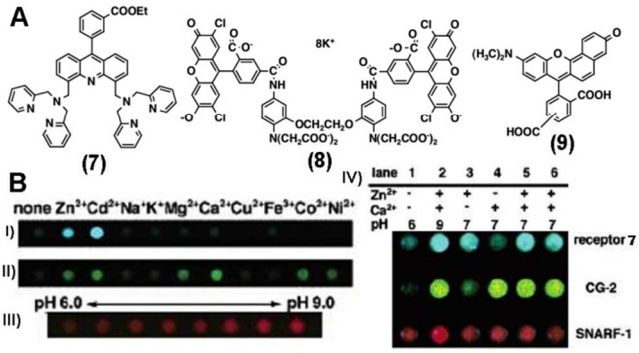

Fig. 5. A) Chemical structure of receptor **7**, CG-2 (**8**), SNARF-1 (**9**), B) photographs of sensing patterns of a semi-wet chemo-sensor chip containing (I) **7** and (II) CG-2 in the presence of various metal cations or (III) SNARF-1 at various pHs, (IV) A photograph of an integrated molecular recognition hydrogel chip for mixed solution assay: **7**, CG-2, or SNARF-1 from the top to bottom. Six mixed solutions including $[Zn(NO_3)_2]$ 0 (-) or 120 μM (+), $[Ca(NO_3)_2]$ 0 (-) or 1 mM (+), pH 6.0, 7.0, or 9.0

The semi-wet environment in supramolecular hydrogel was also amendable to artificial receptors without loss of their molecular recognition capability. The supramolecular hydrogel could therefore be developed by Hamachi and co-workers into a sensor chip for the detection of molecular recognition events.[38]

They demonstrated that the spaces of micrometer-size in the gel could be potentially used as a suitable cavity for molecular recognition. Moreover, the present hydrogel was transparent that spectroscopic analysis of the events inside the gel matrix could be readily carried out. The heated solution (10 μL) containing the gelator (**6**) mentioned in Fig. 4A and different artificial receptors (Fig. 5A) was spotted on a glass plate prior to gelation and stood for 1h to yield a hydrogel array. Upon using different kinds of artificial receptors, high-throughput analysis for Zn^{2+} (Fig. 5B-I) and Ca^{2+} (Fig. 5B-II) could be achieved, where strong fluorescence revealed the presence of the Zn^{2+} and Ca^{2+}, respectively. When a pH probe (SNARF-1) was encapsulated in the supramolecular hydrogel, the pH value could also be visulized by the intensity of the red fluorescence (Fig. 5B-III).

An integrated molecular recognition chip could also be prepared by immobilizing the multiple chemosensors. As shown in Fig.5B-IV, upon integrating the above mentioned three probes into the gel, three distinct analytes (Zn^{2+}, Ca^{2+}, and pH) could be simultaneously analyzed from the mixed solution. For instance, when the mixed solution containing Zn^{2+}, and Ca^{2+} at basic pH was put on the gel spots of the lane 2, three probes emit the corresponding fluorescence in response to the correct guest without being disturbed by other analytes. Furthermore, good coincidence of the binding selectivity and signal changes in the integrated molecular recognition chip was confirmed by the results of lanes 3-6 as smear spots clearly correspond to the missing component (lanes 3-5) or pH shift (lane 6). These observations indicated that the integrated supramolecular sensor chip could be potentially applied to mixed sample analysis without tedious isolation processes.

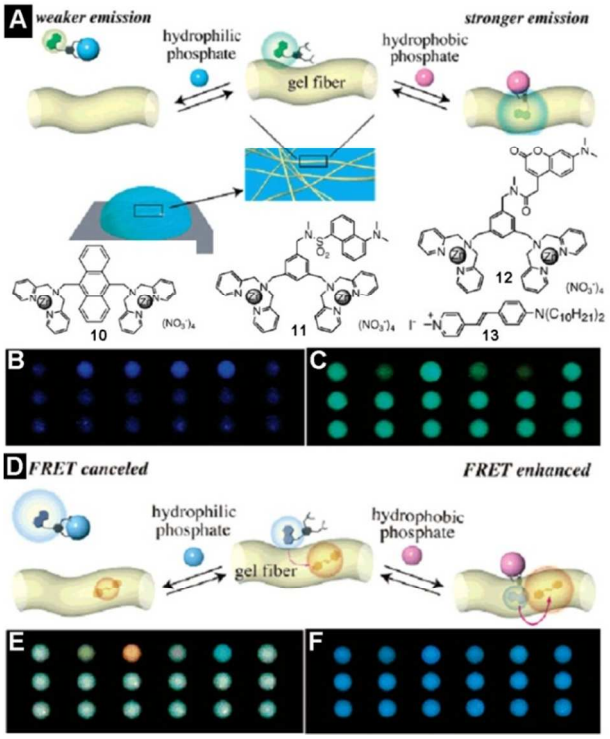

Fig. 6. A) Schematic illustration of the chemosensor redistribution upon the binding to a hydrophobic or hydrophilic phosphate derivative between the hydrophobic domain of nanofiber and the hydrophilic cavity in gel, B) Digital camera photographs of the sensing patterns of semi-wet molecular recognition (MR) chips of the hydrogel containing the bis-Zn/Dpa-anthracene **10** and C) the dansyl-appended receptor **11** in the presence of various anions, D) Illustration of the guest-dependent FRET system using **12** and **13** by the addition of PhP or ATP in the hydrogel matrix, E) Digital camera photographs of the sensing patterns of semi-wet MR chips of the hydrogel containing the coumarin-appended receptor **12** with the styryl dye **13**, and F) **12** without **13** in the presence of various anions (The spotted positions of anions in Fig. 6B-C and Fig. 6E-F from top to bottom are: row 1) receptor only, phosphate, Php, phospho-Tyr, ATP, Me_2P; row 2) Ph_2P, cAMP, Suifate, Carbonate, Nitrate, Acetate; and row 3) Fluoride, Chloride, Bromide, Azide, Glucose, Acetyl choline)

The binding of analytes can change the distribution of fluorescent sensors between the aqueous cavity in gel and the hydrophobic domain in nanofiber, thus altering their fluorescence property. For instance, the binding of a hydrophobic analyte to the sensor will draw the sensor from the solution phase to the hydrophobic domain of nanofibers. Based on this principle, Hamachi and co-workers developed a molecular recognition (MR) device for sensing and discriminating phosphate derivatives.[39] As shown in Fig. 6A, the receptor almost uniformly dispersed in the hydrogel before the host-guest interaction, while it could dynamically change the location from the aqueous cavity to the hydrophobic domain of fibers upon the hydrophobic phosphate binding, resulting in a stronger emission. On the other hand, the receptor remained in the aqueous space of the hydrogel upon the hydrophilic phosphate binding. In this case, only weak emission could be observed.

They then prepared a semi-wet MR chip. When the MR chip containing the PET-type chemosensor **10**, the intensified blue fluorescence at the spots including phosphate, PhP, ATP, and phospho-Tyr could be distinguished from spots including other anions but could not be discriminated from each other (Fig. 6B). However, in the case of the dansyl-appended receptor **11**, the changing pattern of above phosphate derivatives was different from that of chemosensor of **10**. As shown in Fig. 6C, an intensified blue emission was observed at the spot containing PhP, whereas a greenish emission was observed at the spot including ATP, phosphate or phospho-Tyr, which made it possible to easily discriminate phosphate derivatives from each other by visual observations.

The guest-dependent redistribution of the artificial receptor could be extended to the rational construction of a fluorescence resonance energy transfer (FRET) type of read-out system in the semi-wet supramolecular hydrogel. As shown in Fig. 6D, the receptor redistribution upon guest-binding should alter the distance between the fluorescent receptor and the added fluorophore so as to cause a seesaw type of fluorescence change. A coumarin-appended receptor **12** for phosphate derivatives as a FRET donor and a hydrophobic styryl dye **13** as an acceptor were embedded in the supramolecular hydrogel. As shown in Fig. 6E, the color of the hydrogel changed from purplish to orange at the spot of the PhP addition, or to bluish at the spot of the ATP addition, whereas no distinct color change was observed in the absence of **13** (Fig. 6F). Thus the elaborate utilization of the hydrophobic fibrous domains, as well as the water-rich hydrophilic cavities of the supramolecular hydrogel could produce three distinct signal transduction modes: a PET type, an environmentally sensitive type, and a FRET type of fluorescent signal transduction. These studies may lead to versatile and useful chips to screen many important analytes.

3. Self-assembled nanoparticles, nanofibers, micelles for detection applications

Signaling molecules such as fluorophores, fluorine-containing molecules, or contrast agents can be easily conjugated with self-assembling small molecules to yield functional nano-materials. The fluorescence and F-NMR signals are greatly different between self-assembled and un-assembled stages. For example, a self-assembling small mocelule with a conventional fluorophore displays no or only weak fluorescence when assembled due to the aggregation caused quenching (ACQ) effect, whereas it will emit bright fluorescence in response to the target analytes through the recognition-induced dis-assembly.[28] Such big differences in fluorescence and F-NMR signals have been applied for rapid detection of proteins and enzymes.

3.1 Dis-assembly induced signal turn on

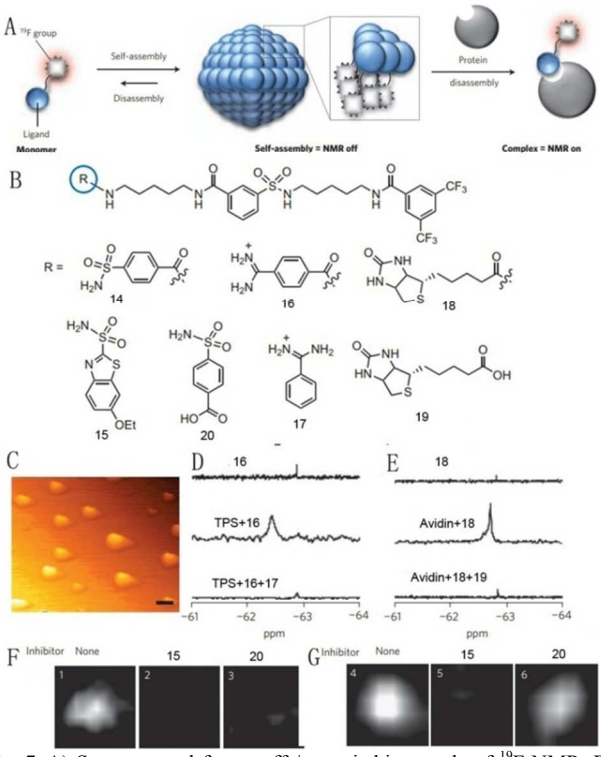

Fig. 7. A) Strategy used for an off /on switching mode of ^{19}F NMR, B) Chemical structures of probes **14**, **16** and **18** for hCAI, TPS and avidin, respectively and chemical structures of enzyme inhibitors **15** and **20** for hCAI, **17** for TPS and ligand **19** for avidin, C) AFM image of the self-assembled probe **14** (scale bar is 500 nm), D) Detection of TPS by turn-on ^{19}F NMR signal of probe **16** and E) Detection of avidin by turn-on ^{19}F NMR signal of probe **18,** and using magnetic resonance images (^{19}F) to detect proteins in red blood cells: F) probe **14** to detect hCAI and G) probe **16** to detect TPS

The ^{19}F-NMR signal of fluorine containing small molecules is silent upon self-assembled stages, while it will recover when dis-assembled. Such dis-assembly triggered ^{19}F-NMR signal turn on had been utilized by Hamachi and co-workers to develop functional nano-materials for the detection of specific proteins.[40] As shown in Fig. 7A, self-assembling small molecular probes composed of a ^{19}F-containing group and a ligand specific to the protein of interest were designed and sythesized. The probe alone was NMR-silent because of its self-assembly, but gave a distinct ^{19}F signal in response to the target protein through the binding-mediated dis-assembly of the probe. In particular, three different probes **14**, **16**, and **18** for their corresponding proteins of human carbonic anhydrase I (hCAI), trypsin(TPS), and avidin, respectively were designed. In the NMR spectroscopy, almost no signal was detected in the buffer solution containing **14**, **16**, or **18** alone, whereas a new signal was intensified on the addition of hCAI, TPS, or avidin, respectively (Fig. 7D). For the control compound **15** (or **20**), **17**, or **19**, such signal intensifications did not occur due to the lack of protein binding ligands. Similarly, the biotin-tethered probe **18** showed a clear off/on response to a non-enzymatic protein, avidin in the ^{19}F NMR spectroscopy(Fig. 7E).

They also showed that probe **14** was capable of detecting hCA within live cell. As shown in Fig. 7F, a distinct ^{19}F-NMR image was obtained from sample 1 due to the recongnition-mediated dis-assembly of the nano-materials. In the presence of inhibitors (samples 2 and 3), no such signals could be observed. Similar to nanoprobe **14**, probe **16** also exhibited a distinct ^{19}F-NMR image upon protein binding while no signal in the presence of inhibitors. Stimulated by this pioneering work, our group also developed nanospheres of F-containing peptides that could respond to the enzyme of tyrosinase for its detection.[41] The oxidation of tyrosine led to the dis-assembly of the nanostructures, resulting in a F-NMR signal turn on. Due to the extremely low abundance of F in human body, ^{19}F-NMR silent nano-materials may provide distinct signals for the *in vivo* detection of different kinds of diseases such as cancer.

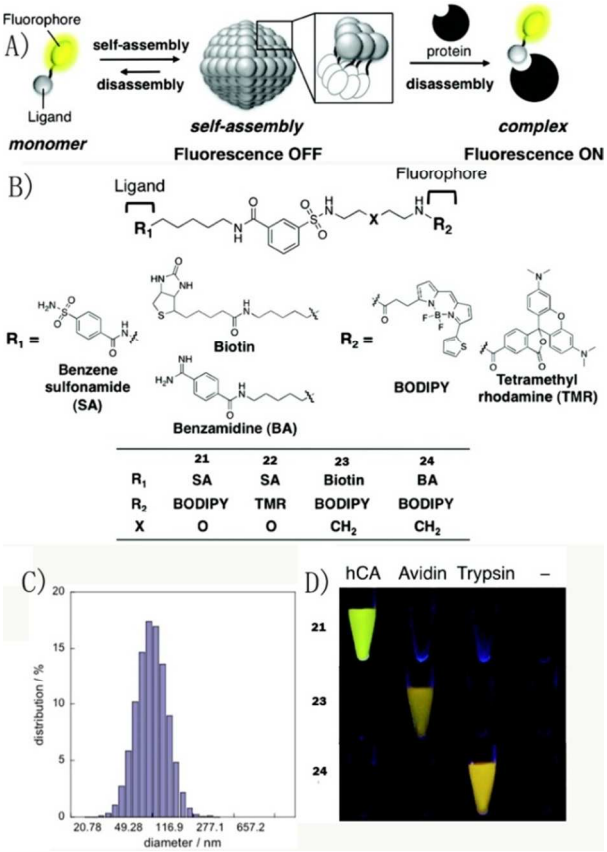

Fig. 8. A) Dis-assembly based strategy for specific protein detection with dis-assembly induced turn-on fluorescent probes, B) Chemical structures of fluorescent probes **21** and **22** for hCA, **23** for avidin, and **24** for trypsin, C) DLS analysis of the particle size distribution of self-assembled probe **21**, D) Photographs showing the orthogonal, specific protein detection of

hCA, avidin, and trypsin using probes **21**, **23**, and **24**, respectively (images were obtained with UV excitation (λ_{ex} = 365 nm))

Using the similar strategy, Hamachi and co-workers introduced "turn on" fluorescent probes that were selective to target proteins.[22] The role of 'disaggregation' has been actively applied to develop optical probes recently.[28] Generally, the fluorophore emitted weakly in nanospheres due to aggregation caused quenching, while emit strongly in response to the target protein through the recognition-induced dis-assembly of the probe (Fig. 8A). They designed the compounds containing ligands of benzene sulfonamide (**21** and **22**), biotin (**23**), and benzamidine (**24**) for the target proteins of hCA, avidin, and trypsin, respectively (Fig. 8B). As designed, the emission was extremely weak [the fluorescence quantum yield (Φ) was 0.001] when **21** assembled in aqueous buffer but dramatically increased (by 38-fold) upon the addition of hCA (Φ =0.04). The enhanced fluorescence of **21** was almost completely quenched again by the addition of EZA, a strong competitive inhibitor of hCA (Fig. 8D). Similar fluorescence turn on phenomenon was observed for nanoprobes **23** and **24** to their coresponding target proteins. None of the probe **21**, **23**, or **24** responded to the non-target proteins, demonstrating the high orthogonality and target specificity of these probes. Such supramolecular approach may facilitate the development of protein-specific turn on fluorescent probes that are useful for a wide range of applications, such as diagnosis and molecular imaging.

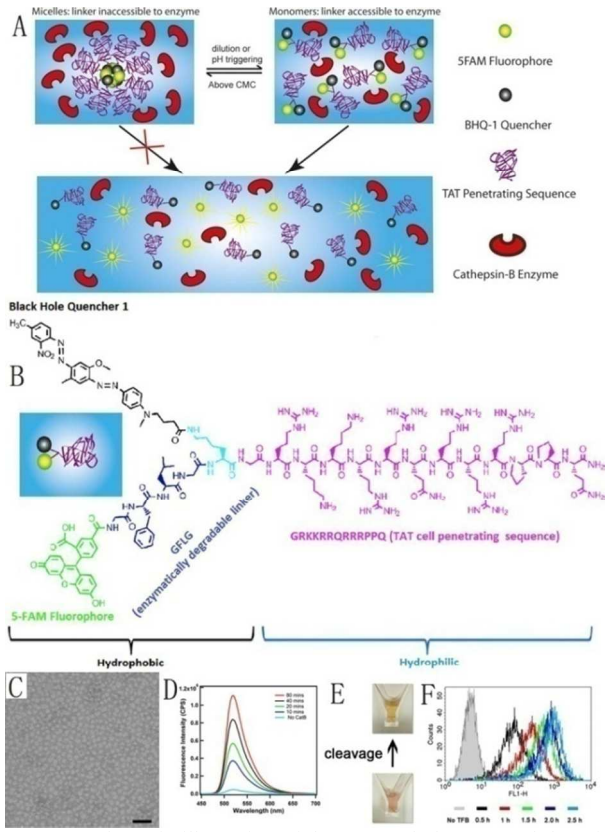

Fig. 9. A) Schematic illustration of the expected cleavage and detection mechanism, B) Molecular structure of the designed nano-beacon molecule TFB, C) TEM images of 200 μM TFB in PBS solutions, D) Time-course fluorescence measurements of a 3 μM TFB PBS solution in the presence of 1 μM CatB, E) photographs of NB solutions before and after CatB cleavage, F) Flow cytometry confirms the increased fluorescence intensity with time inside live MCF-7 cells

Traditional design on peptide-based molecular beacons often leads to their poor stability and facile degradation by non-specific enzymes, resulting in a limitation for accurate detection of enzymatic activities. Such non-specific enzymatic digestion would be greatly attenuated in self-assembled nanoprobes, because the peptide bonds could be deeply buried in the inner core of nano-materials that were not accessible to enzymes. Taking this property, Cui and co-workers rationally developed a novel type of supramolecular nanobeacon that was resistant to non-specific enzymatic degradation on the self-assembled stage but could be effectively cleaved by the target enzyme in the monomeric form.[42] The nanobeacon molecules were specifically designed to self-assemble into core-shell micells, with the enzyme-sensitive design feature being deeply embedded within the micellar core and thus unaccessible to the enzyme (Fig. 9A). As shown in Fig. 9B, the self-assembling molecule consisted of a hydrophobic quencher called black hole quencher (BHQ-1), and a green dye, 5-carboxyfluorescein (5-FAM) onto a hydrophilic peptide, HIV-1 derived cell penetrating peptide, Tat_{48-60}. The cleavable linker that bridged 5-FAM and the lysine N-terminus was a peptide tetramer of Gly-Phe-Leu-Gly (GFLG), which could be effectively cleaved by cathepsin B (CatB), The designed molecule could self-assemble into spherical micelles under physiological condition and above their CMCs (Fig. 9C). Upon accumulation in the tumor microenvironment or entering the lysosomes that were known to be acidic, the nanobeacon would gradually dissociate to individual molecules due to dilution or/and pH triggering, thereby exposing the cleavable linker to the CatB. Eventually, the release of 5-FAM and fluorescence turn on could be used as an indicator for the presence of CatB (Fig. 9D). Importantly, MMP-2 could not show noticeable cleavage reaction to the nanobeacon. They also showed that the nanobeacon molecules could be effctively uptook by live MCF-7 cells and emited a continuous increase in fluorescence with prolonged incubation time (Fig. 9F). These results clearly revealed the big potential of self-assembled nanobeacons for imaging enzyme activity in live cells and for tumor imaging in live animal.

3.2 Self-assembly induced signal turn on

In contrast to conventional fluorescent dyes that possess dis-assembly induced fluorescence turn on property, agregation-induced emission (AIE) dyes and environment sensitive dyes would emit more intensly at assembled stages. For example, the tetraphenylethene (TPE)-based probes are well-known to be weakly fluorescent when being well soluble in aqeuous solution, while its fluorescence can be significantly switched on upon aggregated due to the mechanism of restriction of intramolecular rotations (RIR).[29] For the environment-sensitive fluorophores, they show weak fluorescence in polar environments due to the charge-transfer-induced fluorescence quenching but will exhibit intense fluorescence in hydrophobic environments by reducing charge transfer between the fluorophore and polar media. This light-up strategy has provided new opportunities for the detection of biologically important events with high sensitivity and good signal-to-back ground ratios. The AIE-based probes was recently

reviewed by Tang and co-workers[29] and we only summarized recent progresses in the development of probes based on environment-sensitive fluorescent dyes.

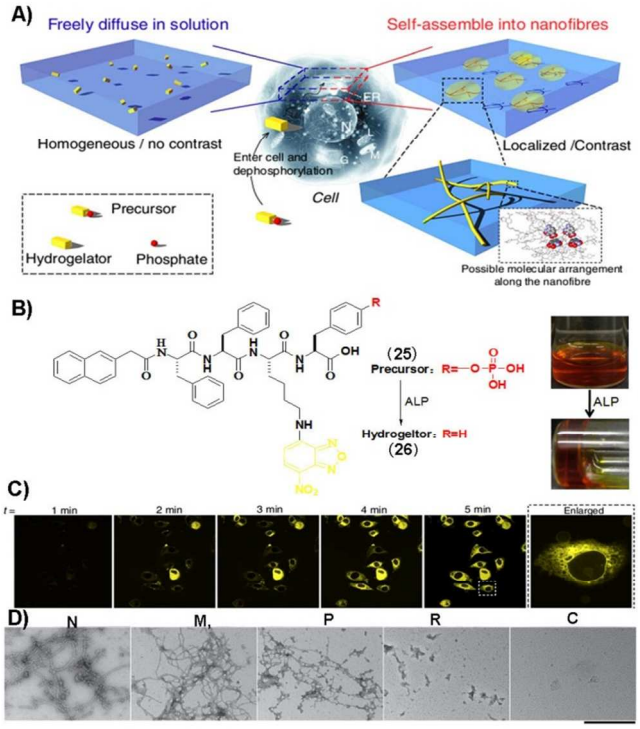

Fig. 10. A) Principle of imaging enzyme-triggered supramolecular self-assembly inside cells, B) Chemical structure of hydrogelator and the hydrogel of **26** by treating **25** with ALP at pH 7.4, C) Fluorescent confocal microscope images showed the time course of fluorescence emission inside the HeLa cells incubated with 500 μM of 20 in PBS buffer (Scale bar, 50 μm for time course panels and 10 μm for the enlarged panels), D) TEM images of each fraction of HeLa cells that were preincubated with **25** for 1 h (Scale bar is 500 nm). Pellet sample N, nuclei; pellet sample M, mitochondria, lysosomes, peroxisomes; pellet sample P, plasma membrane, microsomal fraction (fragments of ER), large polyribsomes; pellet sample R, ribosomal subunits, small polyribosomes; sample C, soluble portion of cytoplasm (Cytosol).

Recently, Xu and co-workers had combined the advantages of high efficiency of enzyme-catalyzed self-assembly and high sensitivity of environment-sensitive fluorescent dyes to develop a method for imaging enzyme-triggered self-assembly of small molecules inside live cells.[43] As shown in Fig. 10A, the precursor of the hydrogelator (NapFFK(NBD)pY (**25**)), bearing an environment-sensitive fluorophore (4-nitro-2,1,3-benzoxadiazole, NBD) and an enzyme trigger (tyrosine phosphate, pY) dissolved well in water and diffused freely, resulting in the homogeneous distribution of the fluorophore. Such evenly distribution afforded little contrast for imaging in confocal microscopy upon being excited. After an enzymatic conversion inside the cell, the precursor turned to the corresponding hydrogelator (**26**) which self-assembled to form nanofibers. Since NBD was a fluorophore that gave more intense fluorescence in a hydrophobic environment than in water, the self-assembly of **26** resulted in nanofibres that fluoresced much brighter than the rest of unassociated molecules of **25** or **26**. Therefore, compound **26** was a valid candidate for studying molecular self-assembly of small molecules inside cells. As shown in Fig. 20C, after the addition of **25** (500 μM) to the cell culture medium, the dynamics of self-assembly of **26** inside live cells was observed in real time by recording the fluorescent images of the cells at different time points. The cells incubated with **25** became slightly fluorescent within 80s, and a bright fluorescent area appeared near the nucleus in one of the cells after 3 min. After 5 min, all the cells glowed brighter at the center of the cytoplasm than around the outer membrane of the cells. The TEM images of the fractions N, M and P of the treated cell showed substantial amount of nanofibers, suggesting the formation of the nanofibers inside cells (Fig. 10D). This significant work, not only establishes a general strategy to provide the spatiotemporal profile of the assemblies of small molecules in cellular environment but may lead to a paradigm for regulating cellular functions and controlling the fate of cells.

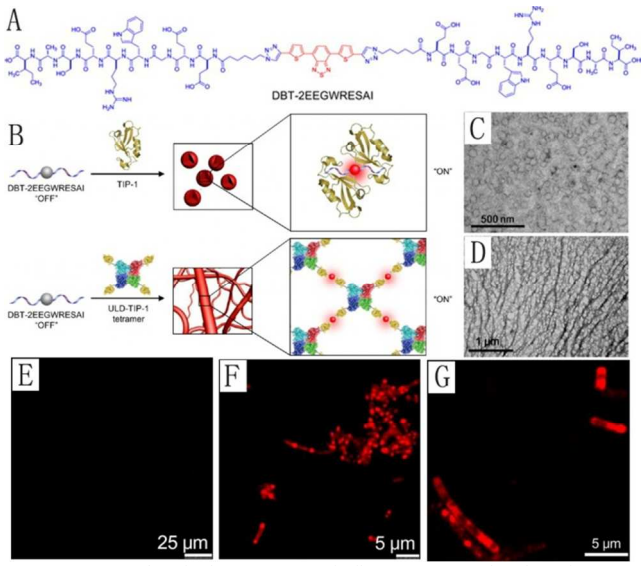

Fig. 11. A) Chemical structure of fluorescent molecule of DBT-2EEGWRESAI, B) Proposed principle of self-assembly-induced FR/NIR fluorescence light-up for detection and visualization of protein/polyprotein peptide interactions based on DBT-2EEGWRESAI, TEM image of C) DBT-2EEGWRESAI after treatment with TIP-1 and D) DBT-2EEGWRESAI after treatment with ULD-TIP-1, Confocal images of live bacteria E) without inducing TIP-1 expression after incubation with DBT-2EEGWRESAI for 4 h, F) after TIP-1 expression and the probe incubation for 4 h, and G) after ULD-TIP-1 expression and the probe incubation for 4 h

Introducing hydrophobic moieties to proteins would change their surface property from hydrophilic to hydrophobic, leading to their aggregations. Taken this strategy and the fluorescence turn on property of environment sensitive probes, we designed and synthesized a far-red/near-infrared (FR/NIR) fluorescence light-up probe (DBT-2EEGWRESAI) for detecting and visualizing specific protein-peptide interactions (Fig. 11A).[44] We firstly demonstrated that 4,7-di(thiophen-2-yl)-2,1,3-benzothiadiazole (DBT) was an environment-sensitive fluorophore with FR/NIR fluorescence due to its strong charge transfer character in the excited state. The specific peptide ligand of WRESAI to the tax interacting protein-1 (TIP-1) was chosen to conjugate with DBT by click chemistry. The resulting probe DBT-2EEGWRESAI was wekly fluorescent in aqueous solution, but lighted up its fluorescence when the probe specifically binded to TIP-1 protein or the tetrameric protein of ULD-TIP-1 (Fig.

11B). It was found that the DBT-2EEWRESAI/TIP-1 protein and the DBT-2EEWRESAI/ULD-TIP-1 tetramer could self-assemble into spherical nanocomplexes and nanofibers, respectively. The formation of nano-structures provided DBT a hydrophobic micro-environment, leading to FR/NIR fluorescence turn-on. By virtue of the self-assembly-induced FR/NIR fluorescence turn-on, DBT-2EEWRESAI could be applied to detect and visualize specific protein/polyprotein-peptide interactions in both solution and live bacteria in a high contrast and selective manner (Fig. 11C). In light of its simplicity, high effectiveness, and high specificities, replacing EEGWRESAI with other peptide ligands may afford a series of FR/NIR fluorescent probes for studying other specific protein/polyprotein-peptide interactions.

4. Summary and outlook

During the last two decades, the preparation and application of self-assembling supramolecular nano-materials have attracted extensive research interests, and it is relative easy to design small molecules that could form nanostructures now.[45] The efforts have now focused on the development of functional nano-materials of them. Due to the rapid responsive property to external stimuli and good biocompatilility of supramolecular nano-materials, they are very promising as nanoprobes to detect environmentally and biologically important analytes with good selectivity and sensitivity.

However, the development of self-assembled supramolecular probes is still in its infant stage and there are still many challenges remained. Though sol-gel/gel-sol transitions of supramolecular hydrogels can be easily observed by naked eyes and thus provide a simple assay for the screening of analytes of interests, the sensitivity of this system is relatively low and the concentration of enzymes or other analytes needs to be high enough to achieve the sol-gel/gel-sol transitions. The development of super-gelators that can form gels at ultra-low concentrations[46, 47] or using polymer additives that can improve the self-assembly ability of small molecules[48, 49] may increase the sensitivity in such detection. The combination of hydrogelators containing AIE/environment-sensitive fluorophores and the strategy of 'surface-induced hydrogelation'[50] may also lead to the generation of assays with improved sensitivity. The integration of a quencher and a fluorescent dye in one supramolecular hydrogelator may lead to a 'super-quenching' effect due to both the ACQ effect and the presence of the quencher. It may lead to the development of versatile hydrogel or paper-based sensor chips that allow to detect analytes by dramatical fluorescence turn on. The examples of self-assembled nanoprobes with turn on F-NMR signal are rare, and research efforts in developing such probes may lead to highly sensitive probes for *in vivo* applications due to the low abundance of fluorine in human body. In situ formation of fluorescent nanofibers offers a unique platform to study enzyme activity insides cells in a highly spatiotemporal manner, which needs to be studied and explored in further steps. Due to the existence of vast specific interactions in nature, binding induced self-assembly/aggregation and fluorescence turn on provide a versatile and useful strategy to design smart probes to visualize important specific interactions. We believe that the research efforts paid to address these problems and challenges would ultimately lead to novel applications of supramolecular nano-materials, new tools to manipulate and imaging biological individuals, and products for practical applications.

We acknowledge the financial supports from National Natural Science Foundation of China (51222303 and 51373079).

Notes and references

[a]*State Key Laboratory of Medicinal Chemical Biology, College of Life Sciences, and Collaborative Innovation Center of Chemical Science and Engineering (Tianjin), Nankai University, Tianjin 300071, P. R. China; E-mail: yangzm@nankai.edu.cn*
[b]*Department of Cardiology, Zhujiang Hospital of Southern Medical University, Guangzhou 510280, P. R. China*

1. G. M. Whitesides and B. Grzybowski, *Science*, 2002, **295**, 2418-2421.
2. Z. Dong, Q. Luo and J. Liu, *Chem. Soc. Rev.*, 2012, **41**, 7890-7908.
3. H. Xu, W. Cao and X. Zhang, *Acc. Chem. Res.*, 2013, **46**, 1647-1658.
4. H. Wei, R.-X. Zhuo and X.-Z. Zhang, *Prog. Polymer Sci.*, 2013, **38**, 503-535.
5. H. Jiang and F.-J. Xu, *Chem. Soc. Rev.*, 2013, **42**, 3394-3426.
6. Q. He, Y. Cui and J. Li, *Chem. Soc. Rev.*, 2009, **38**, 2292-2303.
7. P. Posocco, S. Pricl, S. Jones, A. Barnard and D. K. Smith, *Chem. Sci.*, 2010, **1**, 393-404.
8. A. Barnard and D. K. Smith, *Angew. Chem. Int. Ed.*, 2012, **51**, 6572-6581.
9. J. Boekhoven, A. M. Brizard, K. N. Kowlgi, G. J. Koper, R. Eelkema and J. H. van Esch, *Angew. Chem. Int. Ed.*, 2010, **49**, 4825-4828.
10. M. Reches and E. Gazit, *Science*, 2003, **300**, 625-627.
11. W. Cao, X. Zhang, X. Miao, Z. Yang and H. Xu, *Angew. Chem. Int. Ed.*, 2013, **52**, 6233-6237.
12. G. Liang, H. Ren and J. Rao, *Nat. Chem.*, 2010, **2**, 54-60.
13. J. H. Collier, J. S. Rudra, J. Z. Gasiorowski and J. P. Jung, *Chem. Soc. Rev.*, 2010, **39**, 3413-3424.
14. M. Suzuki and K. Hanabusa, *Chem. Soc. Rev.*, 2009, **38**, 967-975.
15. X. Zhao and S. Zhang, *Chem. Soc. Rev.*, 2006, **35**, 1105-1110.
16. M. Zelzer and R. V. Ulijn, *Chem. Soc. Rev.*, 2010, **39**, 3351-3357.
17. L. A. Estroff and A. D. Hamilton, *Chem. Rev.*, 2004, **104**, 1201-1217.
18. Z. Yang, G. Liang and B. Xu, *Acc. Chem. Res.*, 2008, **41**, 315-326.
19. H. Wang, Z. Yang and D. J. Adams, *Mater. Today*, 2012, **15**, 500-507.
20. F. Zhao, M. L. Ma and B. Xu, *Chem. Soc. Rev.*, 2009, **38**, 883-891.
21. M.-P. Chien, A. S. Carlini, D. Hu, C. V. Barback, A. M. Rush, D. J. Hall, G. Orr and N. C. Gianneschi, *J. Am. Chem. Soc.*, 2013, **135**, 18710-18713.
22. K. Mizusawa, Y. Ishida, Y. Takaoka, M. Miyagawa, S. Tsukiji and I. Hamachi, *J. Am. Chem. Soc.*, 2010, **132**, 7291-7293.
23. J. S. Rudra, T. Sun, K. C. Bird, M. D. Daniels, J. Z. Gasiorowski, A. S. Chong and J. H. Collier, *Acs Nano*, 2012, **6**, 1557-1564.
24. Y. Kuang and B. Xu, *Angew. Chem. Int. Ed. Engl.*, 2013, **52**, 6944-6948.
25. S. M. Standley, D. J. Toft, H. Cheng, S. Soukasene, J. Chen, S. M. Raja, V. Band, H. Band, V. L. Cryns and S. I. Stupp, *Cancer Res.*, 2010, **70**, 3020-3026.
26. R. Cabot and C. A. Hunter, *Chem. Soc. Rev.*, 2012, **41**, 3485-3492.
27. L. Yuan, W. Lin, K. Zheng, L. He and W. Huang, *Chem. Soc. Rev.*, 2013, **42**, 622-661.

28. D. Zhai, W. Xu, L. Zhang and Y.-T. Chang, *Chem. Soc. Rev.*, 2014, **43**, 2402-2411.
29. D. Ding, K. Li, B. Liu and B. Z. Tang, *Acc. Chem. Res.*, 2013, **46**, 2441-2453.
30. Y.-D. Zhuang, P.-Y. Chiang, C.-W. Wang and K.-T. Tan, *Angew. Chem. Int. Ed.*, 2013, **52**, 8124-8128.
31. M. Sainlos, W. S. Iskenderian and B. Imperiali, *J. Am. Chem. Soc.*, 2009, **131**, 6680-6682.
32. S. S. Babu, V. K. Praveen and A. Ajayaghosh, *Chem. Rev.*, 2014, **114**, 1973-2129.
33. G. Blum, G. von Degenfeld, M. J. Merchant, H. M. Blau and M. Bogyo, *Nat. Chem. Biol.*, 2007, **3**, 668-677.
34. Z. Yang and B. Xu, *Chem. Commun.*, 2004, 2424-2425.
35. S. C. Bremmer, J. Chen, A. J. McNeil and M. B. Soellner, *Chem. Commun.*, 2012, **48**, 5482-5484.
36. X. D. Xu, B. B. Lin, J. Feng, Y. Wang, S. X. Cheng, X. Z. Zhang and R. X. Zhuo, *Macromol. Rapid Commun.*, 2012, **33**, 426-431.
37. S. Kiyonaka, K. Sada, I. Yoshimura, S. Shinkai, N. Kato and I. Hamachi, *Nat. Mater.*, 2004, **3**, 58-64.
38. I. Yoshimura, Y. Miyahara, N. Kasagi, H. Yamane, A. Ojida and I. Hamachi, *J. Am. Chem. Soc.*, 2004, **126**, 12204-12205.
39. S. Yamaguchi, I. Yoshimura, T. Kohira, S.-i. Tamaru and I. Hamachi, *J. Am. Chem. Soc.*, 2005, **127**, 11835-11841.
40. Y. Takaoka, T. Sakamoto, S. Tsukiji, M. Narazaki, T. Matsuda, H. Tochio, M. Shirakawa and I. Hamachi, *Nat. Chem.*, 2009, **1**, 557-561.
41. J. Gao, Y. Shi, Y. Wang, Y. Cai, J. Shen, D. Kong and Z. Yang, *Org. Bioorg. Chem.*, 2014, **12**, 1383-1386.
42. L. L. Lock, A. G. Cheetham, P. Zhang and H. Cui, *ACS nano*, 2013, **7**, 4924-4932.
43. Y. Gao, J. Shi, D. Yuan and B. Xu, *Nat. Commun.*, 2012, **3**, 1033.
44. H. Wang, J. Liu, A. Han, N. Xiao, Z. Xue, G. Wang, J. Long, D. Kong, B. Liu and Z. Yang, *ACS Nano*, 2014, **8**, 1475-1484.
45. J. H. van Esch, *Langmuir*, 2009, **25**, 8392-8394.
46. H. Wang, C. Yang, M. Tan, L. Wang, D. Kong and Z. Yang, *Soft Matter*, 2011, **7**, 3897-3905.
47. P. H. J. Kouwer, M. Koepf, V. A. A. Le Sage, M. Jaspers, A. M. van Buul, Z. H. Eksteen-Akeroyd, T. Woltinge, E. Schwartz, H. J. Kitto, R. Hoogenboom, S. J. Picken, R. J. M. Nolte, E. Mendes and A. E. Rowan, *Nature*, 2013, **493**, 651-655.
48. Y. J. Adhia, T. H. Schloemer, M. T. Perez and A. J. McNeil, *Soft Matter*, 2012, **8**, 430-434.
49. G. Pont, L. Chen, D. G. Spiller and D. J. Adams, *Soft Matter*, 2012, **8**, 3797-3802.
50. A. M. Bieser and J. C. Tiller, *Chem. Commun.*, 2005, 3942-3944.

